J Mater Sci (2009) 44:4531–4538
DOI 10.1007/s10853-009-3685-3

Nucleation and growth mechanism of apatite on a bioactive and degradable ceramic/polymer composite with a thick polymer layer

Jeong-Cheol Lee · Sung Baek Cho · Seung Jin Lee · Sang-Hoon Rhee

Received: 7 May 2009 / Accepted: 12 June 2009 / Published online: 23 June 2009

Abstract Nucleation and growth mechanism of apatite on a bioactive and degradable PLLA/SiO_2–CaO composite with a thick PLLA surface layer were investigated compared to that on a bioactive but non-degradable polyurethane (PU)/SiO_2–CaO composite with a thick PU surface layer. The bioactive SiO_2–CaO particles were made by a sol–gel method from tetraethyl orthosilicate and calcium nitrate tetrahydrate under acidic condition followed by heat treatment at 600 °C for 2 h. The PLLA/SiO_2–CaO and PU/SiO_2–CaO composites were then prepared by a solvent casting method which resulted in thick PLLA and PU surface layers, respectively, due to precipitation of SiO_2–CaO particles during the casting process. Two composites were exposed to SBF for 1 week and this exposure led to form uniform and complete apatite coating layer on the PLLA/SiO_2–CaO composite but not on the PU/SiO_2-CaO composite. These results were interpreted in terms of the degradability of the polymers. A practical implication of the results is that a post-surface grinding or cutting processes to expose bioactive ceramics to the surface of a composite with a thick biodegradable polymer layer is not required for providing apatite forming ability, which has been considered as one of the pragmatic obstacles for the application as a bone grafting material.

J.-C. Lee
Department of Dental Biomaterials Science and Dental Research Institute, School of Dentistry, Seoul National University, Yeongeon 28, Jongno, Seoul 110-749, Korea

S. B. Cho
Mineral & Materials Processing Division, Korea Institute of Geosciences and Mineral Resources, Kajeong 30, Yuseong, Daejeon 305-350, Korea

S. J. Lee
College of Pharmacy, Ewha Womans University, Daehyun 11-1, Seodaemun, Seoul 120-750, Korea

S.-H. Rhee (✉)
Department of Dental Biomaterials Science, Dental Research Institute, and BK21HLS, School of Dentistry, Seoul National University, Yeongeon 28, Jongno, Seoul 110-749, Korea
e-mail: rhee1213@snu.ac.kr

Introduction

Bioactive glass or glass–ceramics have good osteoconductivity as a result of spontaneous low crystalline carbonate apatite forming capacity in vivo [1, 2]; however, they have not been widely used in the medical field because of their low mechanical reliability with respect to fracture toughness [3, 4]. This problem is not specific to bioactive glass or glass–ceramics, but is a general problem of all ceramics. The only known solution for this problem is to make a composite by combining hard-brittle ceramics with ductile-tough polymers. As a consequence, several methods have been developed to combine bioactive ceramics and polymers [5–19]. Among these, the most frequently used are solvent casting [7, 9, 19] and thermal blending [5, 12] methods when using synthetic polymers as a polymer source. However, some problems originating from different wettabilities have been found when mixing ceramic and polymer phases. One problem is phase separation that occurs at the interface of the two phases, because the ceramic is hydrophilic whereas the synthetic polymer is generally hydrophobic; this phase separation results in a weakening of the composite's mechanical properties. Another problem is the low degree of dispersion of the bioactive ceramic particles in the polymer matrix. To solve these two problems, silane coupling agents are commonly

used to suppress phase separation and improve the degree of dispersion [20].

Another problem commonly experienced when making a ceramic/polymer composite is the occurrence of single polymer layer on the composite surface because the bioactive ceramic particles, with a higher specific gravity than that of polymer, precipitate at the bottom of the composite during the casting process [7, 9, 19]. This has been believed to prevent producing apatite-forming ability of the composite in vivo because the most of the ceramic particles, which have the role to produce apatite forming ability, are not exposed on the composite surface. Meanwhile, the occurrence of single polymer layer on the composite surface is also found with the thermal-blending method [12] because the ceramic is hydrophilic, while the synthetic polymer and air are hydrophobic. Therefore, post-surface grinding or cutting processes are typically used following the preparation of the composite for exposing the bioactive ceramic particles on the composite surface [21, 22]. These are not only complicated and time consuming processes, but also limit the size of the composite. However, if a biodegradable polymer is used when preparing the composite, cracks can be occurred by the degradation of polymer phase and they presumably act as the pathways for the body fluid to penetrate into the composite; this will give a chance to body fluid to contact with bioactive glass particles which exist inside the composite. Consequently, it is likely to result in the apatite formation on the surface of the composite even though it has a thick polymer layer. However, there has been no report on this phenomenon and the surface grinding or cutting processes for exposing the bioactive glass particles to the composite surface are still generally carried out.

In this study, the effect of polymer degradation during the soaking of the composite, consists of bioactive silica based glass and biodegradable polymer, in the SBF was re-examined with the main focus on the nucleation and growth mechanism of apatite. As model systems, PLLA/SiO_2–CaO and PU/SiO_2–CaO composites made by solvent-casting method were used because PLLA and PU are biodegradable and non-degradable polymers, respectively, while SiO_2–CaO ceramic is well-known system to exhibit apatite forming ability in SBF.

Materials and methods

Preparation of specimens

SiO_2–CaO particles were prepared with a starting composition of $70SiO_2 \cdot 30CaO$ in molar ratio, as described in a previous study [23]. The SiO_2–CaO particles were prepared by hydrolysis and polycondensation of tetraethyl orthosilicate (TEOS, Nacalai Tesque) in calcium nitrate tetrahydrate (Nacalai Tesque) and polyethylene glycol (PEG, Aldrich) in aqueous solution. The molecular weight of PEG used in this experiment was about 10,000.

PEG and calcium nitrate tetrahydrate were dissolved in distilled water and concentrated nitric acid (60 wt%, Nacalai Tesque) was then added. TEOS was added to the above solution under stirring. After 20 min, the solution was transferred to a polystyrene box with its top sealed tightly, and kept at 40 °C in a convection oven for gelation and aging for 1 day. The obtained wet gel was immersed in distilled water for 3 h with the distilled water renewed every hour. After the wet gel was dried at 40 °C for 7 days, it was heated at 600 °C for 2 h and then pulverized using a planetary ball mill. Henceforth, the pulverized SiO_2–CaO particles are referred to as SC particles.

The 90PLLA/10SC composite (in wt%) was made by the solvent-casting method. PLLA powder was dissolved in chloroform (4%) after which SC particles were added to the solution. After stirring vigorously for 1 h, the mixture was poured into a Teflon mold and dried under ambient conditions. The 90PU/10SC composite (in wt%) was made as a control using the same preparation method as for the PLLA/SC composite except tetrahydrofuran was used to dissolve the PU powder.

Apatite-forming mechanism

The apatite-forming mechanisms of the two composites were evaluated by their microstructural and ion concentration evolutions in SBF [24]. The SBF was prepared by dissolving reagent grade NaCl, $NaHCO_3$, KCl, $K_2HPO_4 \cdot 3H_2O$, $MgCl_2 \cdot 6H_2O$, $CaCl_2$, and Na_2SO_4 in ion-exchanged distilled water. The solution was buffered at pH 7.4 with tris(hydroxymethyl) aminomethane ($(CH_2OH)_3CNH_2$) and 1 M hydrochloric acid (HCl) at 36.5 °C. Disk-shaped specimens, 12 mm in diameter by 1 mm in thickness, were cut, sterilized under a UV lamp for 30 min, and then soaked in 30 mL of SBF at 36.5 °C for different periods of time. After soaking, the specimens were removed from the solution, gently rinsed with ion-exchanged distilled water, and then dried at room temperature.

Characterization of the specimens

The microstructures of the specimens before and after soaking in SBF were observed by field emission scanning electron microscopy (FE-SEM; S-4700, Hitachi) after sputter-coating with gold for 15 s. The crystalline phases before and after soaking in SBF were evaluated using a thin film X-ray diffractometer (TF-XRD; D8 Discover, Bruker). The atomic concentrations of calcium, phosphorus, and silicon in the SBF were measured by inductively coupled

plasma atomic emission spectroscopy (ICP-AES; Optima-4300 DV, Perkin Elmer) after soaking the specimens for different periods of time in SBF. The SBF pH as a function of incubation time was measured with a pH meter (DK-20, Horiba).

Results

Figure 1 shows the FE-SEM photographs of the (a) PLLA/SC and (b) PU/SC composites. SC particles exposed on the composite surface were not observed in either specimen; only thick PLLA and PU layers were observed. Surface irregularities in the PU/SC composite came from SC particles under the PU surface layer formed by precipitation during the casting process.

Figure 2 shows the TF-XRD diffraction patterns of the PLLA/SC and PU/SC composites. PLLA peaks such as (010), (200), and (203) [25] were observed in the PLLA/SC composite, but peaks from PU or SC particles were not observed.

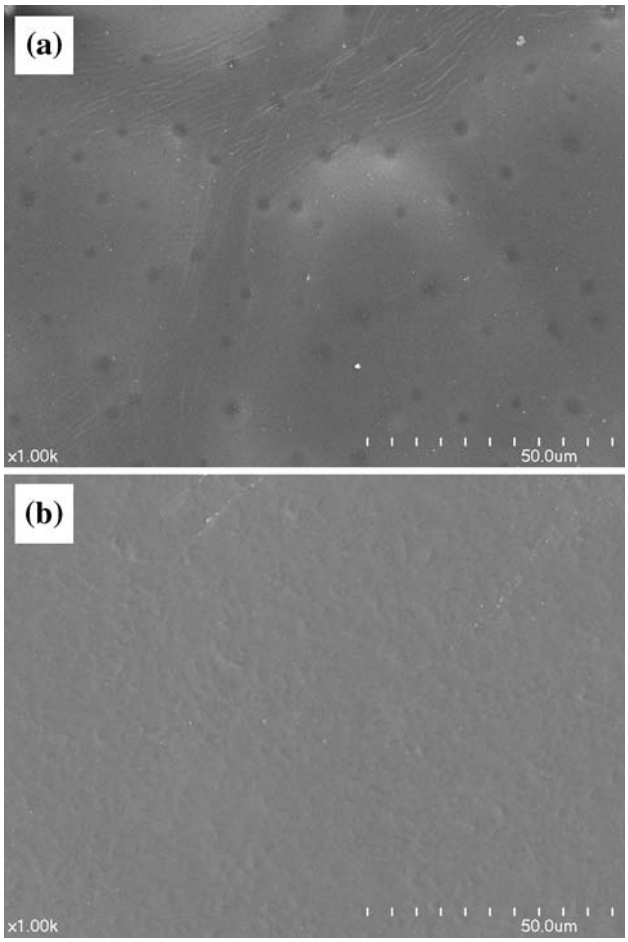

Fig. 1 FE-SEM photographs of as-prepared **a** PLLA/SC and **b** PU/SC composites

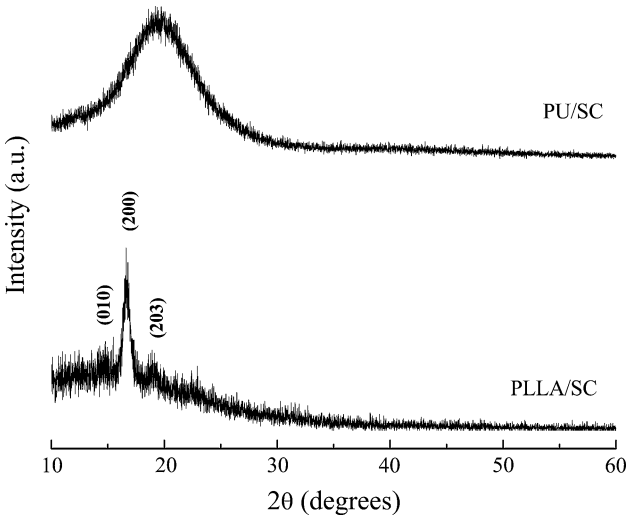

Fig. 2 TF-XRD patterns of the as-prepared PLLA/SC and PU/SC composites

Figure 3 shows the microstructural evolution of the PLLA/SC composite surface after soaking in SBF over time. There were no microstructural changes after 1 day of soaking (Fig. 3a). After 3 days, an uneven distribution of hemispherical-shaped apatite granules, which contain numerous small apatite crystals was observed to occur on the composite surface (Fig. 3b). After 5 days, the number of apatite granules increased (Fig. 3c) and, after 7 days of soaking, granules had spread over the entire composite surface (Fig. 3d, e).

Figure 4 shows the detailed microstructure of Fig. 3b; multiple cracks were found on the PLLA/SC composite surface and apatite crystals formed around these cracks. Underneath the cracks, numerous small apatite crystals were also observed (white arrows). Figure 4b shows the detailed microstructure of the hemispherical-shaped apatite granules in Fig. 4a; these granules contained numerous nano-sized apatite crystals in the size range of about 300–400 nm.

Figure 5 shows the TF-XRD patterns of PLLA/SC composite surfaces after soaking in SBF over time. Apatite peaks denoted by "filled circle (●)" symbols started to occur on day 3 and increased with longer soaking times. This supports the microstructural observations in Fig. 3. Besides the apatite peaks, (200) and (203) PLLA peaks [25] denoted by "open square (□)" symbols were also observed together.

Figure 6 shows the microstructural evolutions of the PU/SC composite surface after soaking in SBF over time. Unlike the PLLA/SC composite shown in Fig. 3, no apatite crystals were observed to form until 14 days of soaking. The initial surface structure was maintained throughout the testing period.

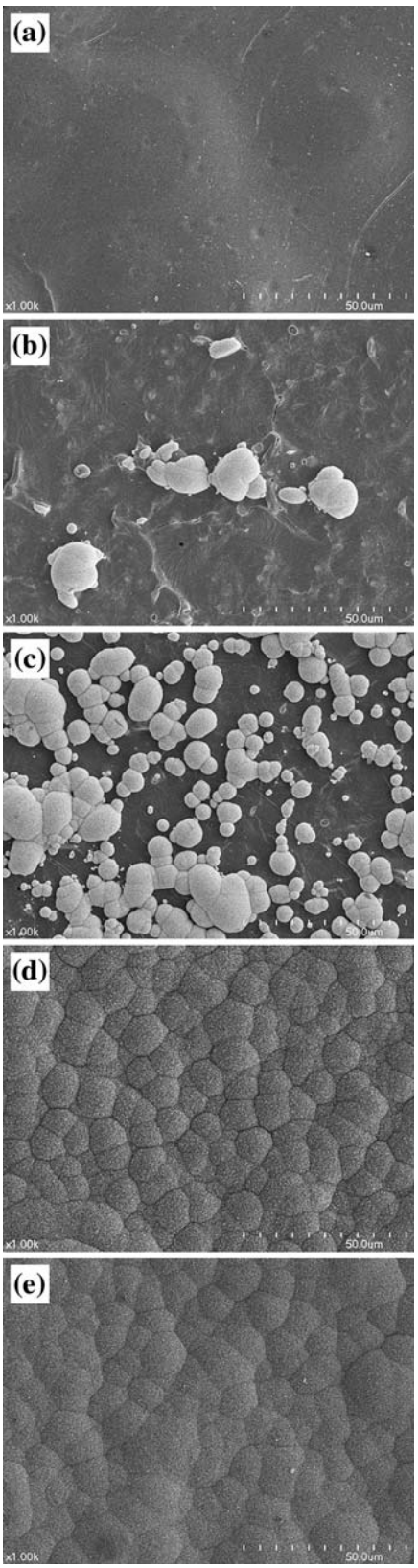

Fig. 3 Microstructural evolutions on the surface of PLLA/SC composite after soaking in SBF for various time periods; **a** 1 day, **b** 3 days, **c** 5 days, **d** 7 days, **e** 14 days

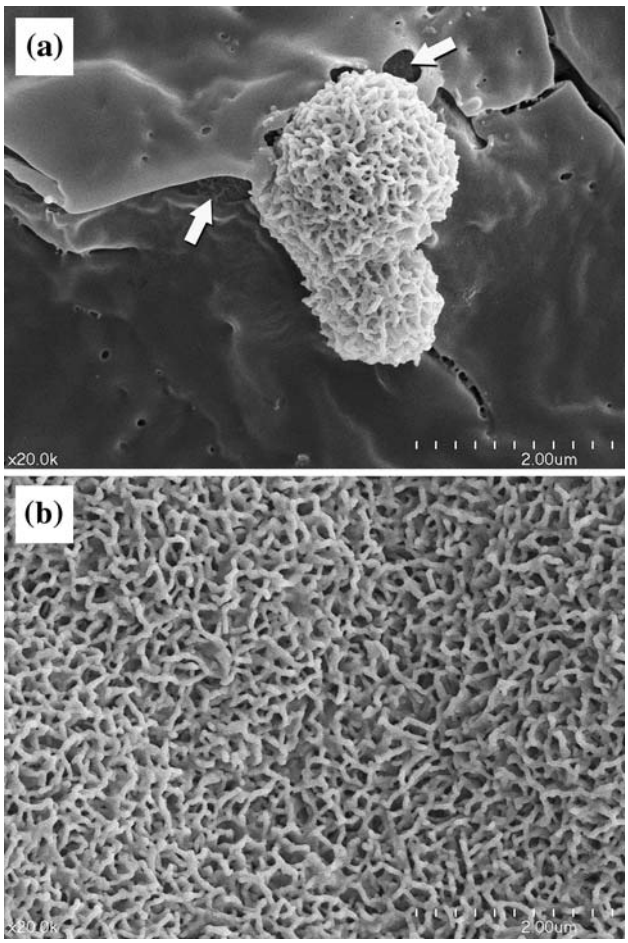

Fig. 4 Detailed microstructures of Fig. 3**b**; **a** the microstructure of apatite granules formed on the crack surfaces and **b** detailed microstructure of the apatite granule in **a**

Figure 7 shows the TF-XRD diffraction patterns of PU/SC composite surfaces after soaking in SBF over time. No peaks except large halo peaks occurred during the testing period. This also supports the microstructural observations shown in Fig. 6.

Figure 8 shows changes in the pH, elemental calcium, phosphorous, and silicon concentrations in the SBF of the two composites after different incubation periods in SBF. The calcium concentration of the PLLA/SC composite reached a maximum after 1 day of soaking but decreased gradually thereafter with longer incubation times. Conversely, the calcium concentration of the PU/SC composite did not undergo any measurable changes within the study period. Similarly, the phosphorous concentration of the PLLA/SC composite decreased slowly until day 3 but thereafter decreased quickly with longer incubation times. In contrast, no significant changes in the phosphorus concentration of the PU/SC composite were observed during the testing period. The silicon concentration followed the same trends as observed for phosphorus; it increased

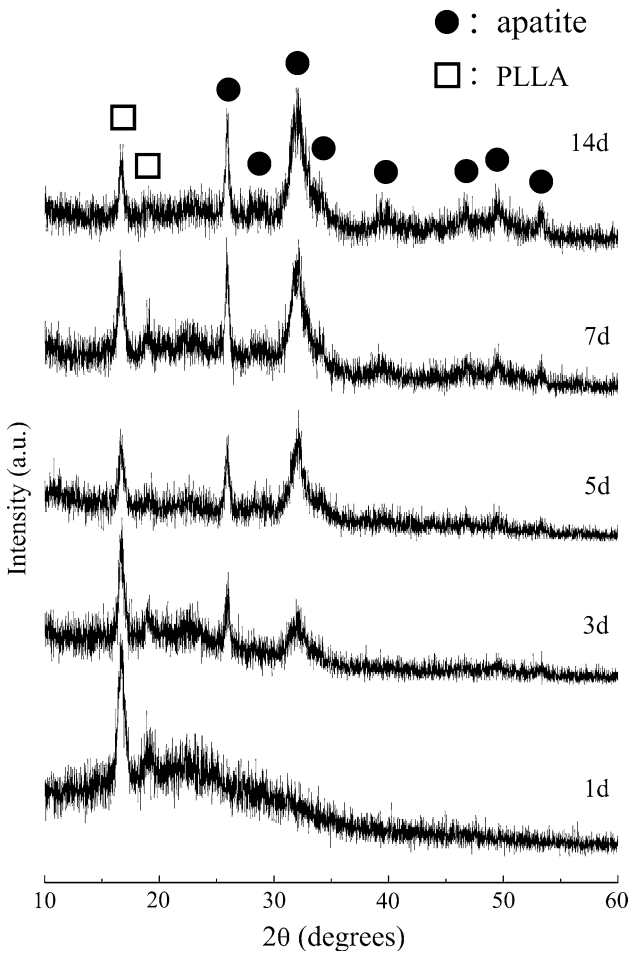

Fig. 5 TF-XRD patterns of PLLA/SC composite after soaking in SBF for various time periods

gradually in the PLLA/SC composite with longer periods of incubation but did not change in the PU/SC composite. The pH of the SBF solution containing the PLLA/SC composite reached a maximum after 3 days and then decreased gradually with longer incubation, while the pH of the SBF solution containing the PU/SC composite remained the same throughout the testing period.

Figure 9 shows the changes in ionic activity products (IAPs) of apatite in SBF due to immersion. In the SBF in which the PLLA/SC composite was soaked, the IAPs reached a maximum after 3 days of soaking and then quickly decreased, but levels of the IAPs did not change appreciably in the PU/SC composite.

Discussion

Presence of a thick polymer layer on the outer surface of a bioactive ceramic/polymer composite formed by the precipitation of incorporated ceramic particles is regarded as a

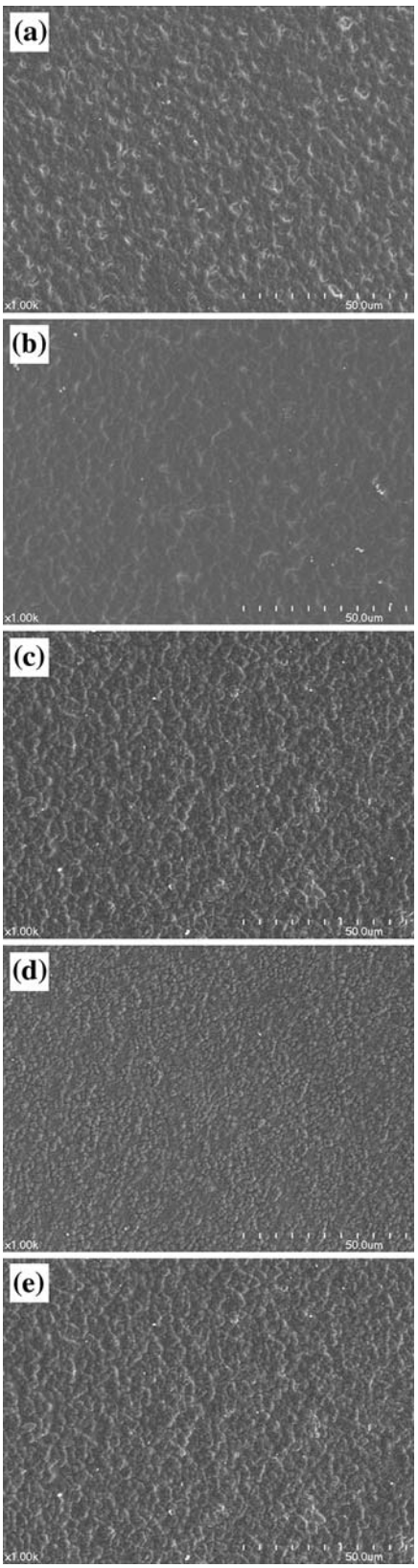

Fig. 6 Microstructural evolutions on the surface of PU/SC composite after soaking in SBF for various time periods; **a** 1 day, **b** 3 days, **c** 5 days, **d** 7 days, **e** 14 days

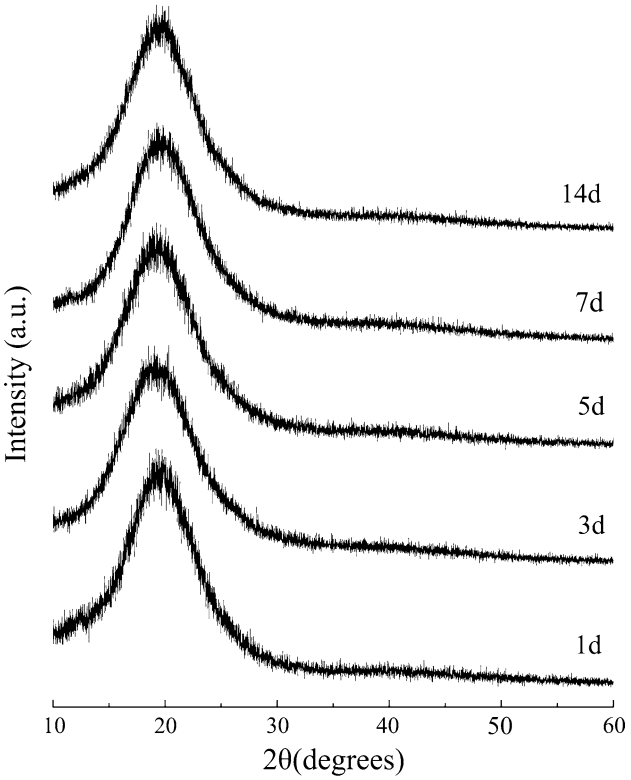

Fig. 7 TF-XRD patterns of PU/SC composite after soaking in SBF for various time periods

limitation for the application as a bone grafting material. This thick polymer layer presumably acts as a barrier to the apatite-forming ability of the bioactive ceramic particles by separating them from body fluid. A solution to this problem has been to remove this thick polymer layer by post-surface grinding or cutting processes that expose bioactive ceramic particles to the composite surface. Following the post-treatment process, exposed bioactive ceramic particles that come directly into contact with body fluid are believed to regain their ability to produce apatite.

In this study, in contrast to existing theory, the PLLA/SC composite with a thick PLLA surface layer produced apatite in SBF, whereas the PU/SC composite with a thick PU surface layer did not. The different apatite-forming potentials of these two composites are thought to be due to surface cracks caused by the degradation of polymer in the PLLA/SC composite.

The initial step in the degradation of a biodegradable polymer is the cleavage of a specific linkage such as an ester group in PLLA [26]. This produces a hydrophilic end group such as carboxyl and hydroxyl groups, which result in swelling of the polymer because of absorption of body fluid, and eventually a cracked surface. Thus, when a composite comprising bioactive ceramic particles and a biodegradable polymer is made by a solvent-casting method, it has the capacity to produce surface cracks because of degradation in the body fluid. The surrounding body fluid will penetrate the surface cracks and contact the bioactive ceramic particles inside the composite. When the bioactive ceramic particles, such as the SC particles in this study, come into contact with SBF, the calcium and silicate ions can dissolve into the body fluid. The released Ca^{2+} ions from silica network produces new silanol groups, which are known to be nucleation sites for the formation of apatite, by exchange of Ca^{2+} ions from SC particles with H_3O^+ ions in the body fluid [27, 28]. This exchange increases the IAP of apatite in body fluid, which promotes the nucleation of apatite on the newly formed silanol groups of SC particles or on the PLLA surface simply by heterogeneous nucleation when supersaturation with respect to apatite becomes high enough. When the released silicate ions adhere to the PLLA surface, they also act as nucleation sites for the formation of apatite crystals [29]. Both mechanisms explain the nucleation of apatite crystals on the non-bioactive PLLA surface in this study. Once the apatite nuclei form on the surfaces of the SC particles and PLLA, they grow spontaneously because the body fluid has been supersaturated with respect to apatite [30].

Surface cracks occurred after 3 days of soaking the PLLA/SC composite in SBF, and apatite crystals first occurred around the surface cracks (Figs. 3b, 4a). The detailed microstructural data in Fig. 4 indicate that the apatite crystals form initially at the SC particles under the thick PLLA layer (white arrows in Fig. 4a) and then grow toward the PLLA surface (two apatite granules on the surface of composite in Fig. 4a). Indeed, the ICP-AES data corroborated this observation (Fig. 8). The calcium and silicon concentrations in the SBF increased with PLLA/SC incubation time, which suggests that the SBF makes contacts with SC particles inside the PLLA/SC composite by penetrating through surface cracks. This also explains the microstructural observations in Figs. 3, 4, and 6. The released calcium elevated the IAP of apatite in SBF (Fig. 9) and helped for the nucleation of apatite on the PLLA/SC composite (Fig. 3). Moreover, the gradual increase in silicon concentration indicates that silicate ions dissolved into the SBF from SC particles became nucleation sites for the formation of apatite on SC particles [27] and on the PLLA surface.

In contrast, no surface cracks were observed during the testing period in the PU/SC composite and likewise, no apatite formation was observed (Figs. 6, 7). Unchanged concentrations of calcium and silicon in the SBF (Fig. 8) and IAP (Fig. 9) also support the SBF having no contact with SC particles.

Based on these results, we conclude that the ability to form apatite can be induced even on the surface of a bioactive and degradable polymer/ceramic composite with a thick polymer layer as a result of crack formation. Thus,

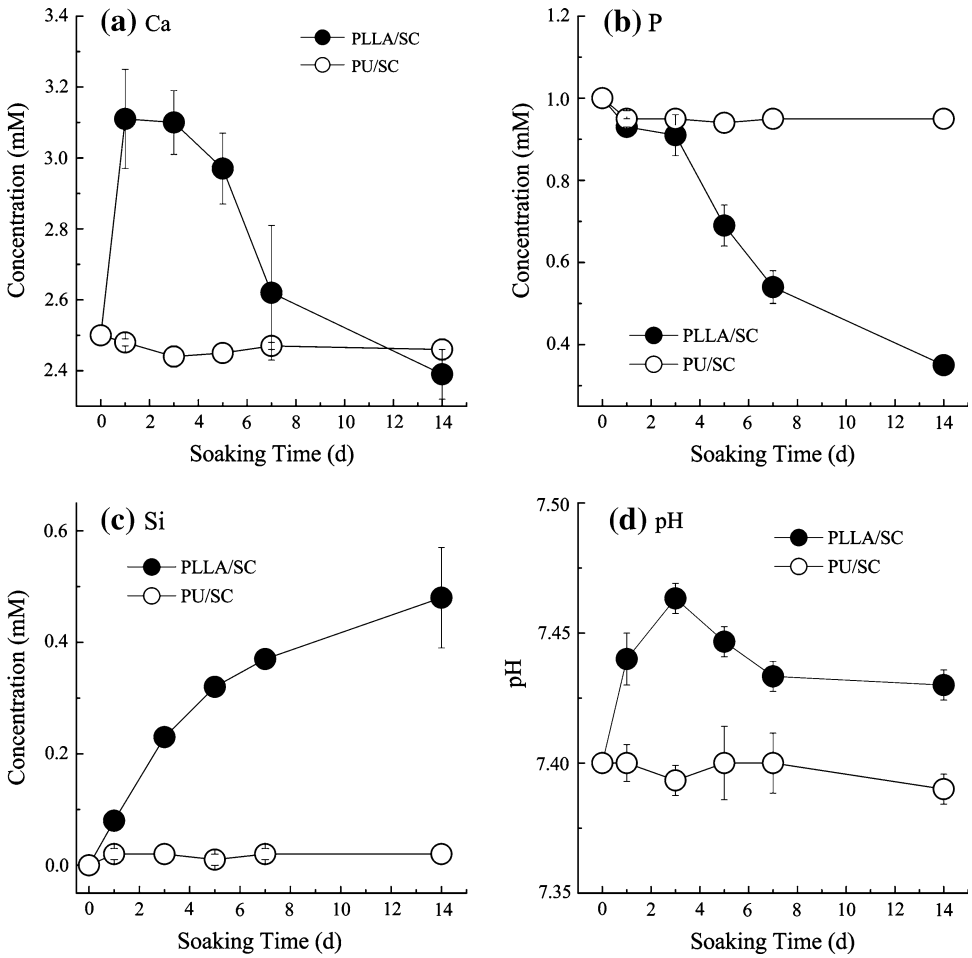

Fig. 8 Changes in pH, elemental calcium, phosphorous, and silicon concentrations in the two composites after different incubation periods in SBF. **a** Ca, **b** P, **c** Si, **d** pH

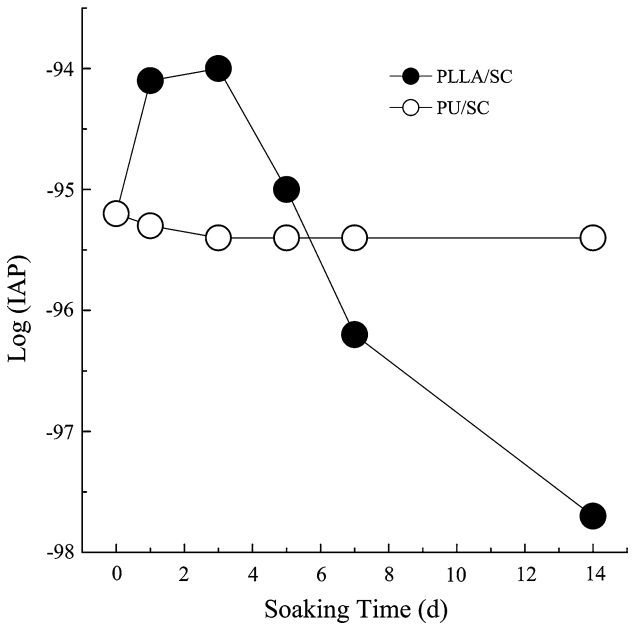

Fig. 9 Changes in IAPs of apatite in SBF due to the immersion of PLLA/SC and PU/SC composites

post-surface grinding or cutting processes to expose the bioactive ceramic particles inside the composite are not needed. It should also be noted that not like the nano-composites made by a sol–gel method, these composites do not have the potentials to release harmful products such as acids or unreacted metal alkoxides that can originate from non-heat-treatment processes involved in the sol–gel method of formation.

Conclusions

PLLA/SC composites with a thick and biodegradable PLLA surface were shown to have apatite-forming ability without the need for a post-surface grinding or cutting process. This apatite-forming ability is presumably due to SBF penetration through surface cracks caused by the degradation of the PLLA surface layer and contact with SC particles inside the composite. In contrast, apatite did not form on PU/SC macrocomposites with a thick PU surface layer because no surface cracks formed during treatment with SBF. Together, these results suggest that apatite

crystals can form on composites with a thick and biodegradable polymer layer even without a post-surface treatment process.

Acknowledgement This work was supported by the Nano Bio R&D Program (Platform technologies for organ/tissue regeneration (Regenomics), Grant No. M0528010001-06N2801-00110) of the Korea Science & Engineering Foundation.

References

1. Hench LL, Splinter RJ, Allen WC, Greenlee TK Jr (1972) J Biomed Mater Res Symp 2:117
2. Kokubo T, Shigematsu M, Nagashima Y, Tashiro T, Nakamura T, Yamamuro T, Higashi S (1982) Bull Inst Chem Res, Kyoto Univ 60:260
3. Clupper DC, Hench LL, Mecholsky JJ (2004) J Eur Ceram Soc 24(10–11):2929
4. Rawlings RD (1993) Clin Mater 14(2):155
5. Bonfield W, Grynpas MD, Tully AE, Bowman J, Abram J (1981) Biomaterials 2(3):185
6. Taguchi Y, Yamamuro T, Nakamura T, Nishimura N, Kokubo T, Takahata E, Yoshihara S (1990) J Appl Biomater 1(3):217
7. Elgendy HM, Norman ME, Keaton AR, Laurencin CT (1993) Biomaterials 14(4):263
8. Kawanabe K, Tamura J, Yamamuro T, Nakamura T, Kokubo T, Yoshihara S (1993) J Appl Biomater 4(2):135
9. Jansen JA, de Ruijter JE, Janssen PTM, Paquay YGCJ (1995) Biomaterials 16(11):819
10. Piattelli A, Franco M, Ferronato G, Santello MT, Martinetti R, Scarano A (1997) Biomaterials 18(8):629
11. Du FZC C, Zhu XD, de Groot K (1999) J Biomed Mater Res 44(4): 407
12. Kikuchi M, Tanaka J, Koyama Y, Takakuda K (1999) J Biomed Mater Res 48(2):108
13. Peter SJ, Lu L, Kim DJ, Mikos AG (2000) Biomaterials 21(12):1207
14. Bleach NC, Nazhat SN, Tanner KE, Kellomäki M, Tömälä P (2002) Biomaterials 23(7):1579
15. Rhee S-H, Choi JY, Kim HM (2002) Biomaterials 23(24):4915
16. Kamitakahara M, Kawashita M, Miyata N, Kokubo T, Nakamura T (2002) J Mater Sci: Mater Med 13(11):1015
17. Rhee S-H, Lee Y-K, Lim B-S, Yoo JJ, Kim HJ (2004) Biomacromolecules 5(4):1575
18. Wei G, Ma PX (2004) Biomaterials 25(19):4749
19. Kim S-S, Sun Park M, Jeon O, Yong Choi C, Kim B-S (2006) Biomaterials 27(8):1399
20. Beatty MW, Swartz ML, Moore BK, Phillips RW, Roberts TA (1998) J Biomed Mater Res 40(1):12
21. Okada Y, Kobayashi M, Neo M, Kokubo T, Nakamura T (2001) J Biomed Mater Res 57A(1):101
22. Väkiparta M, Forsback A-P, Lassila LV, Jokinen M, Yli-Urpo AUO, Vallittu PK (2005) J Mater Sci: Mater Med 16(9):873
23. Kim IY, Kawachi G, Kikuta K, Cho SB, Kamitakahara M, Ohtsuki C (2008) J Eur Ceram Soc 28(8):1595
24. Kokubo T, Kushitani H, Sakka S, Kitusgi T, Yamamuro T (1990) J Biomed Mater Res 24:721
25. Nam J, Ray S, Okamoto M (2003) Macromolecules 23(2):634
26. Griffith LG (2000) Acta Mater 48:263
27. Kokubo T, Kushitani H, Ohtsuki C, Sakka S, Yamamuro T (1992) J Mater Sci: Mater Med 3:79
28. Ohtsuki C, Kokubo T, Yamamuro T (1992) J Non-Cryst Solids 143:84
29. Abe Y, Kokubo T, Yamamuro T (1990) J Mater Sci: Mater Med 1:233
30. Neuman WF, Neuman MW (1958) The chemical dynamics of bone mineral. University of Chicago, Chicago